

OPEN

Magnetic Resonance Elastography-derived Stiffness Predicts Renal Function Loss and Is Associated With Microvascular Inflammation in Kidney Transplant Recipients

Anwar S. Shatil, MSc,¹ Anish Kirpalani, MSc,^{1,2,3} Eyesha Younus, PhD,^{1,4} Pascal N. Tyrrell, PhD,⁵ Adriana Krizova, MD,⁶ and Darren A. Yuen, MD, FRCPC, PhD^{3,7}

Background. Organ stiffening can be caused by inflammation and fibrosis, processes that are common causes of transplant kidney dysfunction. Magnetic resonance elastography (MRE) is a contrast-free, noninvasive imaging modality that measures kidney stiffness. The objective of this study was to assess the ability of MRE to serve as a prognostic factor for renal outcomes.

Methods. Patients were recruited from the St Michael's Hospital Kidney Transplant Clinic. Relevant baseline demographic, clinical, and Banff histologic information, along with follow-up estimated glomerular filtration rate (eGFR) data, were recorded. Two-dimensional gradient-echo MRE imaging was performed to obtain kidney "stiffness" maps. Binary logistic regression analyses were performed to examine for relationships between stiffness and microvascular inflammation score. Linear mixed-effects modeling was used to assess the relationship between stiffness and eGFR change over time controlling for other baseline variables. A G²-likelihood ratio Chi-squared test was performed to compare between the baseline models with and without "stiffness."

Results. Sixty-eight transplant kidneys were scanned in 66 patients (mean age 56 ± 12 y, 24 females), with 38 allografts undergoing a contemporaneous biopsy. Mean transplant vintage was 7.0 ± 6.8 y. In biopsied allografts, MRE-derived allograft stiffness was associated only with microvascular inflammation (Banff g+ptc score, Spearman $\rho=0.43$, $P=0.01$), but no other histologic parameters. Stiffness was negatively associated with eGFR change over time (Stiffness × Time interaction $\beta=-0.80$, $P<0.0001$), a finding that remained significant even when adjusted for biopsy status and baseline variables (Stiffness × Time interaction $\beta=-0.46$, $P=0.04$). Conversely, the clinical models including "stiffness" showed significantly better fit ($P=0.04$) compared with the baseline clinical models without "stiffness." **Conclusions.** MRE-derived renal stiffness provides important prognostic information regarding renal function loss for patients with allograft dysfunction, over and above what is provided by current clinical variables.

(*Transplantation Direct* 2022;8: e1334; doi: 10.1097/TXD.0000000000001334).

INTRODUCTION

Despite enhancements in short-term renal allograft survival over the last 20 y, long-term outcomes have not similarly

improved.^{1,2} Indeed, although 1-y allograft survival rates are now >90%, 5- and 10-y outcomes have remained significantly lower.¹ Low-grade inflammation may be an important

Received 17 March 2022. Revision received 8 April 2022.

Accepted 12 April 2022.

¹ Department of Medical Imaging, St. Michael's Hospital, Unity Health Toronto, Toronto, ON, Canada.

² Department of Medical Imaging, University of Toronto, Toronto, ON, Canada.

³ Keenan Research Centre for Biomedical Science, St. Michael's Hospital, Unity Health Toronto, Toronto, ON, Canada.

⁴ Department of Medical Physics, Odette Cancer Centre, Sunnybrook Health Sciences Centre, Toronto, ON, Canada.

⁵ Department of Medical Imaging, Department of Statistical Sciences, Institute of Medical Science, University of Toronto, Toronto, ON, Canada.

⁶ Department of Laboratory Medicine and Pathobiology, St. Michael's Hospital, Unity Health Toronto, Toronto, ON, Canada.

⁷ Division of Nephrology, Department of Medicine, St. Michael's Hospital, Unity Health Toronto, University of Toronto, Toronto, ON, Canada.

A.S.S. and A.K. shared cofirst authorship for this article.

A.S.S. and A.K. contributed to concept formulation, data acquisition, data analysis and interpretation, drafting of the article, and final approval for publication. E.Y. and P.N.T. contributed to data acquisition, data analysis, review of the final draft, and final approval for publication. A.K. contributed to performing all allograft biopsies, review of the final draft, and final approval for publication. D.A.Y. contributed to concept formulation, data acquisition, data

analysis and interpretation, supervision of the study, acquisition of the funding, drafting of the article, and final approval for publication.

The authors declare no conflicts of interest.

This work was supported by a Collaborative Health Research Project Grant from the Canadian Institutes of Health Research (CIHR) and the National Sciences and Engineering Research Council of Canada, as well as grants from the Physicians' Services Incorporated Foundation, Astellas Pharma Canada (SG-185), and the St. Michael's Hospital Foundation.

Supplemental digital content (SDC) is available for this article. Direct URL citations appear in the printed text, and links to the digital files are provided in the HTML text of this article on the journal's Web site (www.transplantationdirect.com).

Correspondence: Darren A. Yuen, MD, FRCPC, PhD, 209 Victoria St., 5th Floor, Rm 509, Toronto, ON, Canada M5B 1T8. (darren.yuen@utoronto.ca).

Copyright © 2022 The Author(s). *Transplantation Direct*. Published by Wolters Kluwer Health, Inc. This is an open-access article distributed under the terms of the Creative Commons Attribution-Non Commercial-No Derivatives License 4.0 (CCBY-NC-ND), where it is permissible to download and share the work provided it is properly cited. The work cannot be changed in any way or used commercially without permission from the journal.

ISSN: 2373-8731

DOI: 10.1097/TXD.0000000000001334

contributor to allograft dysfunction, that if left unchecked, progresses to irreversible fibrosis.³⁻⁶ In particular, microvascular inflammation, whether meeting criteria for antibody-mediated rejection or not, is an important cause of allograft damage,⁷⁻¹¹ that can cause capillary leak, tissue edema, and consequent organ stiffening.¹²⁻¹⁴

Magnetic resonance elastography (MRE) is a functional MRI technique that can be used to image organ stiffness.¹⁵ In this technique, an oscillatory pressure source transmits small vibrations through the allograft, whereas synchronized MRI images are used to measure the induced microscopic tissue motion.¹⁵⁻¹⁷ The applied vibratory force and the observed tissue displacement are used to estimate kidney stiffness.

We and others have tested the ability of MRE to identify processes that can affect renal stiffness, and whether MRE-derived information can serve as a prognostic factor for future changes in kidney function.¹⁷⁻¹⁹ In a pilot study of 16 kidney transplant recipients undergoing a for-cause biopsy, for example, we found a modest correlation between MRE-derived allograft stiffness and fibrotic burden.¹⁷ In that preliminary study, MRE-derived stiffness values also correlated with estimated glomerular filtration rate (eGFR) loss over 12 mo, suggesting that MRE might be a useful test to provide additive information regarding future changes in renal allograft function. However, in that small cohort, we were unable to control for important confounding variables. Furthermore, besides fibrosis, microvascular inflammation is also a common and important form of injury seen in dysfunctional allografts. This microvascular inflammation can lead to edema, which might also increase allograft stiffness. To date, however, no MRE study has explored whether microvascular inflammation is associated with allograft stiffening. Therefore, in this study, we hypothesized that MRE-derived allograft stiffness would correlate with microvascular inflammation on a contemporaneous renal biopsy, and be associated with more rapid renal function loss postscan, even when adjusted for important baseline variables.

MATERIALS AND METHODS

Patient Population

Renal allograft recipients >18 y of age were recruited through the Kidney Transplant Clinic at St Michael's Hospital in a prospective cohort study. Our institutional review board approved the study protocol (16-341), which adhered to the Declaration of Helsinki. All participants provided written informed consent. All clinical and research procedures followed the Principles of the Declaration of Istanbul under the Declaration of Istanbul on Organ Trafficking and Transplant Tourism.

Kidney transplant biopsies were performed either for allograft dysfunction, or conducted as part of an independent, parallel clinical trial assessing the effects of high- or low-dose tacrolimus with or without renin-angiotensin system blockade.²⁰ Participants meeting any of the following criteria were excluded: (1) inability or unwillingness to provide informed consent, (2) pregnancy, (3) claustrophobia, (4) contraindication to MRI, (5) <5 mo from time of transplant (to ensure full healing of skin incision), and (6) <3 eGFR data points.

Clinical Data Collection

Baseline age, gender, etiology of primary kidney disease, type of transplant, transplant vintage, diabetes status, rejection

history, serum creatinine, and urine albumin-to-creatinine ratio (ACR) were collected. eGFR was calculated using the Chronic Kidney Disease Epidemiology Collaboration 2009 Equation.²¹ The eGFR and ACR values on or before the date of MRE scan (within 60 d) were collected as baseline data. Patients were followed until the date of major adverse kidney event (MAKE) or study completion (December 31, 2020), whichever occurred first. A MAKE was defined as (1) having 2 consecutive eGFR <15 mL/min measurements at least 30 d apart, (2) return to dialysis or relisting for repeat transplantation, or (3) death from renal causes.

Image Acquisition

MRE was performed on a 3.0 Tesla system (Siemens Skyra, version VD13A), using an 18-channel torso-phased array coil. A flow-compensated fast gradient-echo (GRE) multislice 2-dimensional (2D) MRE sequence was used with motion-encoding gradients applied in the slice-select direction. A paddle connected to an active pneumatic driver was placed over the allograft. Five slices were acquired in the true coronal orientation through the allograft hilum. MRI acquisition parameters included repetition time = 50 ms, echo time = 21 ms, acquisition matrix = 128 × 128, field of view = 30–40 cm², slice thickness = 5 mm, slice gap = 1 mm, vibration frequency = 60.1 Hz, and bandwidth = 601 Hz/pixel. The acquisition time was 4.5 min.

MRE Analyses

A 2D multimodel direct inversion algorithm was used to reconstruct 2D MRE data processed by vendor-supplied built-in software.²² Magnitude, phase, confidence, colorized wave propagation, and elastogram stiffness images representing shear modulus were generated. A stiffness map with 95% confidence was also generated to exclude unreliable regions (Figure 1A). Magnitude images were used to trace the allograft parenchyma, which were later overlaid on the 95% confidence interval (CI) stiffness maps to extract regions of interest (ROIs). The mean stiffness from ROIs spanning a minimum of 3 coronal slices (excluding edge slices) was defined as the mean stiffness of the whole organ. All ROI tracings and calculations were done using ImageJ (v1.53, National Institutes of Health, Bethesda, MD) and MATLAB software version R2018a (The Mathworks, Inc., Natick, MA) by a research analyst (A.S.S.) blinded to the patient's clinical and histopathologic results.

Biopsy Assessment

Ultrasound-guided allograft biopsies were performed within 2 mo after the MRE scans. A blinded renal pathologist (A.K.) analyzed the biopsies and reported Banff scores for glomerulitis (g), peritubular capillaritis (ptc), tubulitis (t), interstitial inflammation (i), intimal arteritis (v), arteriolar hyalinosis (ah), tubular atrophy (ct), interstitial fibrosis (ci), vascular fibrous intimal thickening (cv), and glomerular double contours (cg) according to Banff 2015 criteria.^{23,24} For cases in which a range of scores was provided by the reading pathologist, the mean of the range was used. For example, if a biopsy was scored as t1–t2, a mean score of 1.5 was used.

Statistical Analyses

Descriptive statistics are summarized as mean ± SD for all baseline variables. To assess the relationship between

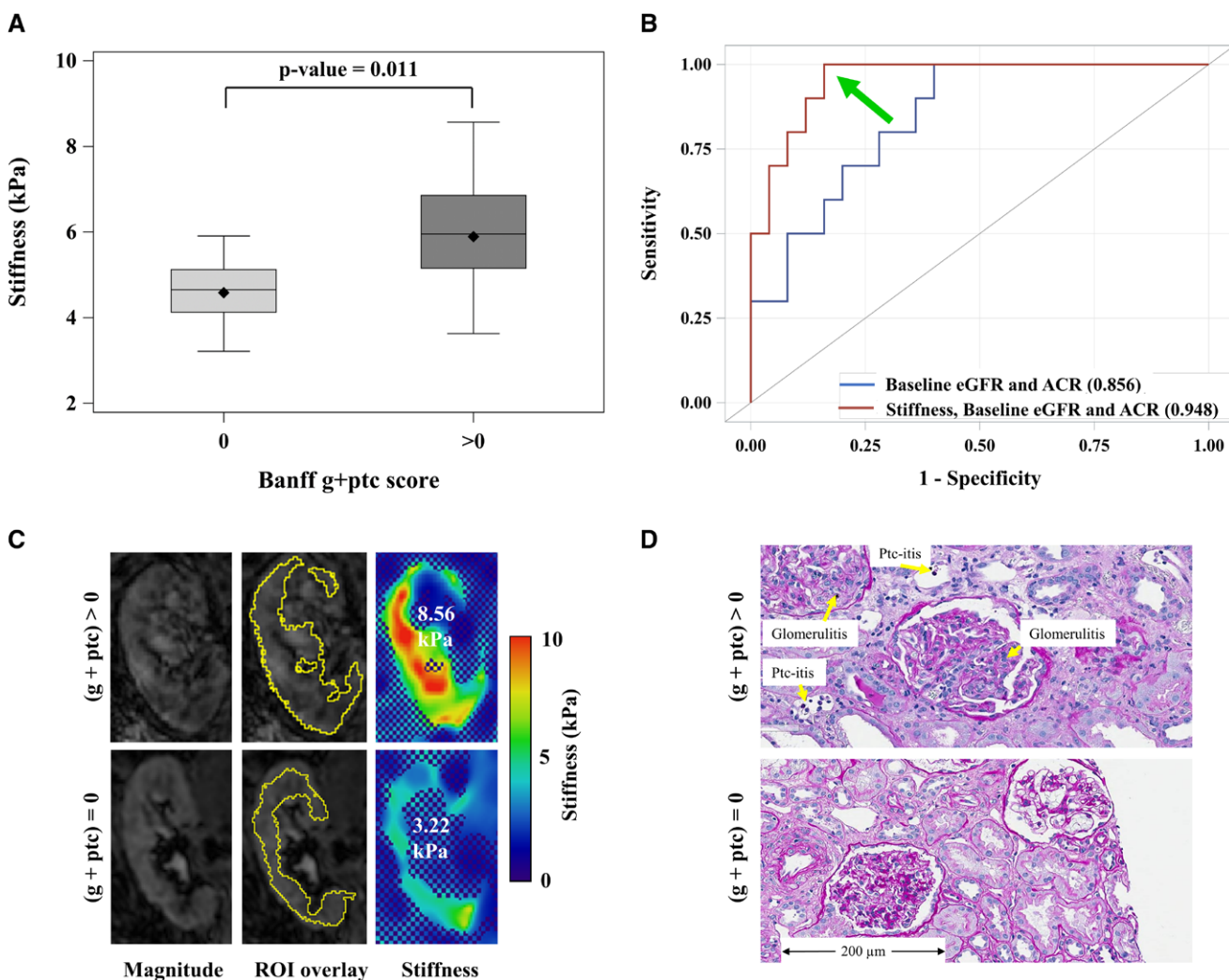


FIGURE 1. Relationships between stiffness and microvascular inflammation. (A) Box plot showing the distribution of MRE-derived stiffness stratified by microvascular inflammation ($g+ptc \geq 0$) with the P value from logistic regression. (B) ROC curves from logistic regression models showing AUC values for a model containing baseline eGFR, baseline urine ACR, and stiffness (AUC 0.948) vs a model containing only baseline eGFR and baseline urine ACR (AUC 0.856) as a prognostic factor for $g+ptc$. (C) Representative magnitude, ROI, and stiffness maps from MRE scans of 2 representative allografts from the cohort showing low stiffness when $g+ptc=0$ and high stiffness when $g+ptc > 0$. Cooler and warmer colors represent softer and stiffer tissues respectively. (D) Corresponding histology of the 2 allografts shows the absence ($g+ptc=0$) and presence ($g+ptc > 0$) of microvascular inflammation. ACR, albumin-to-creatinine ratio; AUC, area under the curve; eGFR, estimated glomerular filtration rate; g, glomerulitis; MRE, magnetic resonance elastography; ptc, peritubular capillaritis; ROC, receiver operating characteristic; ROI, region of interest.

stiffness and Banff scores in biopsied allografts, Pearson and Spearman rank correlations, as well as univariate binary logistic regression analyses, were performed. For the binary logistic regression analyses, Banff scores >0 in any category were assigned a value of “1,” whereas Banff scores of 0 were assigned a value of “0.” For all logistic regressions, odds ratio (OR) and area under curve (AUC) were calculated. The receiver operating characteristic models were compared by using a Chi-squared test.

To calculate annualized eGFR slope, we used clinically collected serum creatinine values, which were performed at least every 3 mo, as per our standard clinic protocol. However, we opted to include only eGFR measurements spaced at a minimum of 1 mo apart, since serum creatinine values can change rapidly and dramatically in the setting of an acute kidney injury event. We reasoned that serum creatinine values collected <1 mo apart would be more likely to reflect acute renal function changes. As eGFR calculations assume that the patient’s kidney function is in steady state, values calculated from these

closely spaced measurements may be less accurate and could skew our analyses. To assess for an independent association between MRE-stiffness and mean annual eGFR slope, a linear mixed-effects analysis was performed, which is known to overcome the limitations of other common approaches.²⁵ We used a stiffness \times time interaction term as a predictor variable, including random slope for time and random intercept in the unadjusted model. The model was adjusted for multiple variables as described in the text. To check whether stiffness adds to the clinically available measurements, a G^2 likelihood ratio statistic was calculated as the difference between $-2\log$ of the baseline models including and excluding stiffness \times time interaction term as a predictor. P value was obtained from the G^2 likelihood ratio Chi-squared test with 3 degrees of freedom. Differences in Akaike information criterion (AIC) were also calculated between the models. All statistical analyses were performed using SAS software version 9.4 (SAS Institute, Cary, NC). A 2-tailed P value <0.05 was defined as statistically significant.

TABLE 1.
Cohort demographics and baseline characteristics

	All	Biopsied	Nonbiopsied
Number of patients	66	36	30
Number of kidney allografts	68	38	30
Female (%)	24 (36)	13 (36)	11 (36)
Age (y)	56 ± 12	55 ± 12	59 ± 12
Transplant vintage (y)	7.0 ± 6.76	4.7 ± 4.2	9.8 ± 8.1
Donor type (living/deceased)	29/39	17/21	12/18
Diabetes status (%)	27 (39)	14 (36)	13 (43)
Rejection history (%)	22 (32)	17 (44)	5 (16)
Baseline eGFR (mL/min/1.73m ²)	32 ± 16	39 ± 19	23 ± 5
Baseline ACR	81 ± 131	97 ± 132	61 ± 128
Number of eGFR data points	911	631	280
Annualized eGFR slope (mL/min/1.73m ² /y)	-3.65 ± 0.75	-4.78 ± 1.13	-2.24 ± 0.73
Whole kidney MRE-derived stiffness (kPa)	4.88 ± 1.12	4.87 ± 1.16	4.89 ± 1.10
Number of allografts experiencing MAKE	25	17	8
Follow-up duration (y)	2.30 ± 1.76	3.00 ± 2.06	1.42 ± 0.53
Cause of end-stage renal disease (number of patients)			
Glomerulonephritis	31	22	9
Polycystic kidney disease	7	4	3
Diabetic nephropathy	7	3	4
Focal segmental glomerulosclerosis	3	3	0
Obstructive uropathy	1	1	0
Others	8	3	5

ACR, albumin-to-creatinine ratio; eGFR, estimated glomerular filtration rate; MAKE, major adverse kidney event; MRE, magnetic resonance elastography.

RESULTS

Clinical Characteristics

Baseline characteristics are summarized in Table 1. A total of 68 transplant kidneys were scanned in 66 patients, of which 2 patients (male=1, female=1) underwent renal transplantation twice. The mean eGFR slope and mean follow-up time for the entire cohort was -3.65 ± 0.75 mL/min/1.73m² per year and 2.30 ± 1.76 y, respectively. Of the 38 biopsied allografts, 29 were clinically indicated for allograft dysfunction, with the remaining 9 kidneys undergoing protocol biopsies as part of a separate trial (see Materials and Methods section for details).²⁰

Biopsy Characteristics

A total of 38 allograft biopsies were performed. A summary of the histologic findings is presented in Table 2. One biopsy

demonstrated acute cellular rejection, 6 had changes suspicious for acute cellular rejection, 2 were consistent with acute antibody-mediated rejection, and 2 were read as mixed acute cellular and acute antibody-mediated rejection. Fourteen biopsies demonstrated interstitial fibrosis and tubular atrophy or other chronic changes without significant inflammation. The remaining 13 biopsies demonstrated other findings, such as recurrent glomerulonephritis or no discernible abnormalities.

Stiffness and Banff Histology Scores

We first assessed for relationships between stiffness and histologic measures of tissue injury in the subset of 38 patients who underwent a contemporaneous renal biopsy. When each Banff category was assessed individually, only glomerulitis (Banff g score) correlated significantly with MRE-derived stiffness (Table S1, SDC, <http://links.lww.com/TXD/A425>, Spearman $\rho=0.48$, $P=0.003$), although peritubular capillaritis also

TABLE 2.
Banff scores of biopsied allografts

	Mean ± SD (n)
Arteriolar hyalinosis (ah)	0.9 ± 0.8 (35)
Glomerular double contours (cg)	0.3 ± 0.7 (35)
Interstitial fibrosis (ci)	1.5 ± 0.8 (37)
Tubular atrophy (ct)	1.5 ± 0.9 (37)
Vascular fibrous intimal thickening (cv)	1.3 ± 1 (36)
Glomerulitis (g)	0.5 ± 1 (35)
Interstitial inflammation (i)	0.5 ± 0.9 (36)
Mesangial matrix increase (mm)	0.6 ± 0.8 (34)
Peritubular capillaritis (ptc)	0.4 ± 0.7 (36)
Tubulitis (t)	0.6 ± 0.8 (35)
Intimal arteritis (v)	0.0 ± 0.1 (36)
Microvascular inflammation (g + ptc)	0.9 ± 0.2 (35)
Nonvascular inflammation (t + i)	1.1 ± 0.2 (35)

TABLE 3.
Association between stiffness and microvascular inflammation (g + ptc)

Models	1	2	3
MRE-stiffness (per kPa)	4.09 (1.37–12.20) ^a		8.28 (1.27–53.93) ^a
Baseline eGFR (per mL/min/1.73m ²)		0.93 (0.85–1.01)	0.91 (0.81–1.03)
Baseline ACR		1.01 (1.00–1.02) ^a	1.014 (1.00–1.03) ^a
Area under curve	0.808	0.856	0.948
P value vs model 2 (Chi-square test)	0.719		0.079

^a $P < 0.005$.

Models 1 and 2 are unadjusted. Model 3 is model 1, with further adjustment for baseline eGFR and baseline ACR.

ACR, albumin-to-creatinine ratio; eGFR, estimated glomerular filtration rate; g, glomerulitis; MRE, magnetic resonance elastography; ptc, peritubular capillaritis.

demonstrated a modest, nonsignificant correlation (Spearman $\rho=0.27$, $P=0.12$). Similarly, when stiffness was used as a variable in a univariate logistic regression model, Banff g score was the only category that was significantly associated with stiffness (OR [95% CI]=5.3 [1.5-18.8], $P=0.01$) with an AUC of 0.85. Banff ptc score demonstrated a modest, nonsignificant association with stiffness (OR [95% CI]=2.0 [0.95-4.36], $P=0.07$). We next generated a composite Banff score reflecting total microvascular inflammation (g+ptc), and found that it positively correlated with stiffness (Spearman $\rho=0.48$, $P=0.003$), whereas stiffness was not associated with nonvascular inflammation (t+i, Spearman $\rho=0.08$, $P=0.628$). Similarly, in univariate logistic regression models, a significant association was observed only between stiffness and g+ptc (Table 3, OR [95% CI]=4.09 [1.37-12.20], $P=0.011$) but not between stiffness and t+i (OR [95% CI]=1.3 [0.7-2.5], $P=0.369$). The association between stiffness and g+ptc remained significant (OR [95% CI]=8.28 [1.27-53.93], $P=0.026$) when the model was adjusted for baseline eGFR and ACR (Figure 1). This model, which included stiffness,

baseline eGFR, and baseline ACR, associated more closely with g+ptc, with a higher AUC (AUC=0.948) compared with a model composed of standard clinical variables alone (baseline eGFR and ACR, AUC=0.856) (Figure 1), a result that neared statistical significance ($P=0.07$). Conversely, stiffness did not significantly associate with t+i when controlled for baseline eGFR and ACR (OR [95% CI]=1.31 [0.7-2.5], $P=0.401$) (Figure 2). Stiffness did not associate with any other Banff histologic parameters (Figure 3; Figures S1 and S2, SDC, <http://links.lww.com/TXD/A425>), although stiffer kidneys did tend to show higher fibrosis scores (Figure S1, SDC, <http://links.lww.com/TXD/A425>).

MRE-derived Allograft Stiffness Is Associated With Future Changes in Renal Function

To assess the clinical relevance of MRE-derived stiffness measurements, we next looked for associations between allograft stiffness and changes in renal function postscan, using a series of linear mixed-effect models (Table 4). In an unadjusted linear mixed-effect model (model 1 in Table 4),

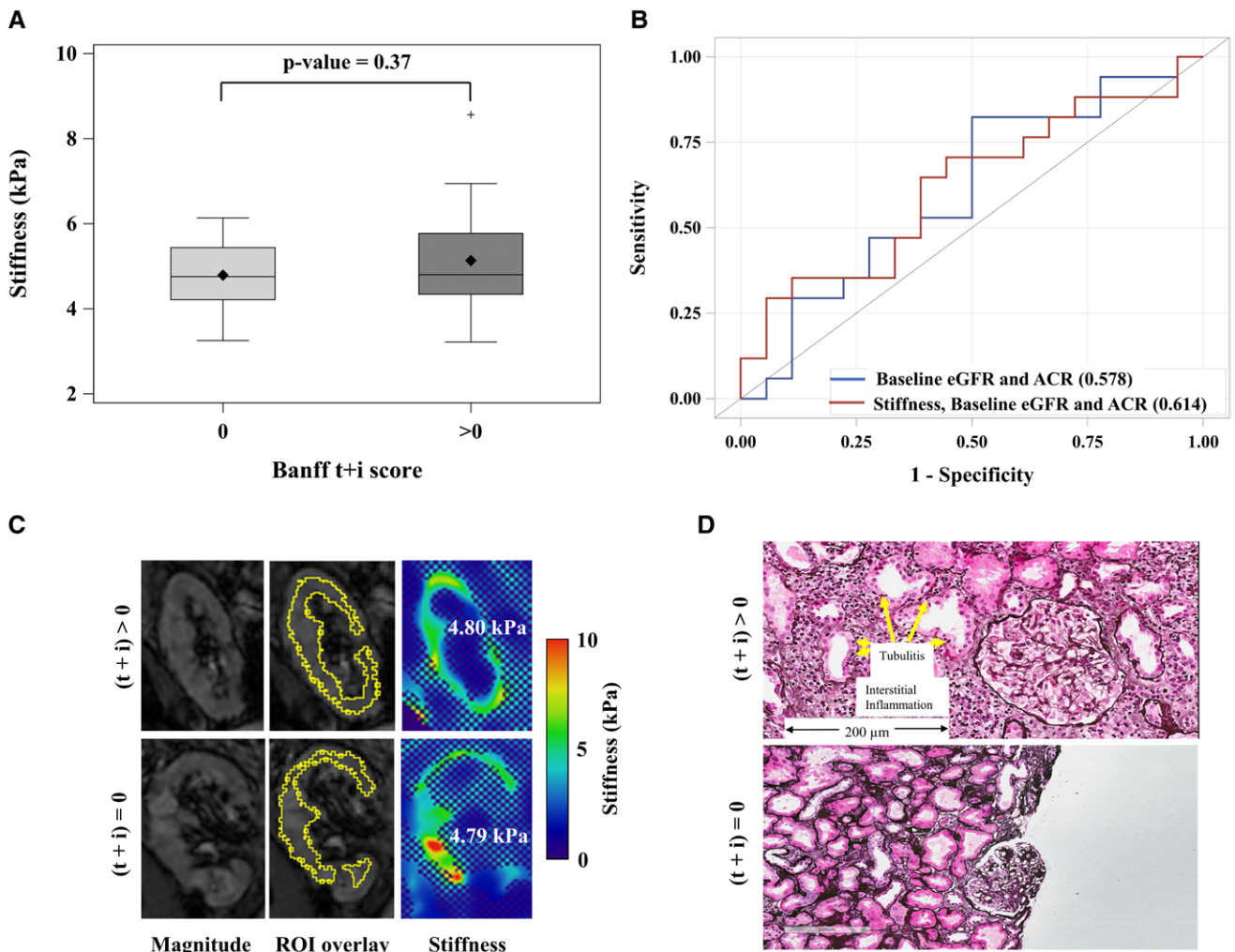


FIGURE 2. Relationship between stiffness and nonvascular inflammation. (A) Boxplot showing the distribution of MRE-derived stiffness stratified by tubular and interstitial inflammation ($t+i \geq 0$) with the P value from logistic regression. (B) ROC curves from logistic regression models using baseline eGFR and baseline urine ACR with (AUC 0.621) and without stiffness (AUC 0.608) as prognostic factors for $t+i$. (C) Representative magnitude, ROI and stiffness maps from MRE scans of 2 kidney allografts from the cohort showing low stiffness when $t+i \geq 0$. Cooler and warmer colors represent softer and stiffer tissues, respectively. (D) Corresponding histology of the 2 allografts showing the absence ($t+i=0$) and presence ($t+i > 0$) of tubulitis and interstitial inflammation. ACR, albumin-to-creatinine ratio; AUC, area under the curve; eGFR, estimated glomerular filtration rate; i, interstitial inflammation; MRE, magnetic resonance elastography; ROC, receiver operating characteristic; ROI, region of interest; t, tubulitis.

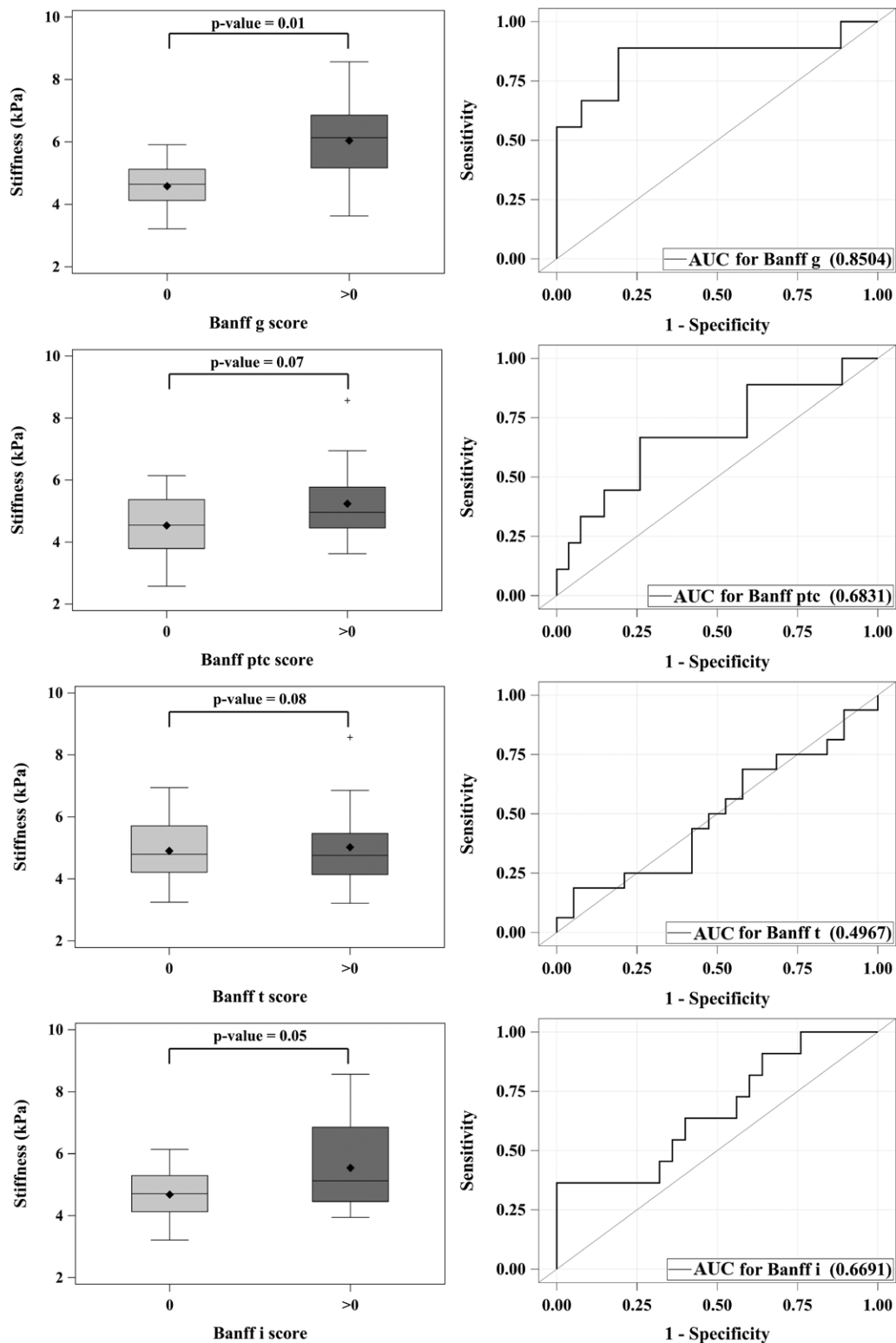


FIGURE 3. Allograft stiffness is increased in kidneys with microvascular inflammation. The figure shows *P* values (left column) and ROC (right column) derived from binary logistic regression analyses comparing histologic scores with stiffness. The corresponding AUC value for each ROC analysis is provided in the bottom right-hand corner of each receiver operating curve. AUC, area under the curve; g, glomerulitis; i, interstitial inflammation; ptc, peritubular capillaritis; ROC, receiver operating characteristic; t, tubulitis.

stiffness was negatively associated with eGFR change over time (stiffness \times time interaction $\beta = -0.80$, $P < 0.0001$, see Figure 4 for representative images). As clinicians currently use baseline renal function and albuminuria to estimate risk of disease progression,^{26,27} we also examined whether stiffness

was associated with these baseline variables. No correlation, however, was found, although stiffness did positively correlate with MAKE (Table S1, SDC, <http://links.lww.com/TXD/A425>, Spearman $\rho = 0.30$, $P = 0.01$). We next generated a model adjusting for baseline eGFR, baseline ACR, baseline

TABLE 4.**Association between stiffness and eGFR change over time using linear mixed-effects modeling**

Models	Estimate of Fixed Effects			
	1	2	3	4
MRE-stiffness (kPa) × Time	-0.80 ^a	-0.50 ^b	-0.46 ^b	-0.47 ^b
Baseline eGFR (mL/min/1.73m ²)	0.86 ^a	0.87 ^a	0.87 ^a	0.88 ^a
Baseline ACR		-0.007	-0.007	-0.008
Baseline ACR × time		-0.02 ^c	-0.02 ^c	-0.02 ^c
Follow-up time		1.54 ^c	1.62 ^c	1.56 ^c
Biopsy status			-0.57	-0.25
Biopsy status × time			-0.34	-0.33
Age (y)				0.06
Gender				-0.36
Diabetes status				1.07
Rejection history				0.13

^a*P* < 0.0001.^b*P* < 0.05.^c*P* < 0.005.

Model 1 is unadjusted. Model 2 is adjusted for baseline eGFR, ACR, baseline ACR × time interaction and follow-up time. Model 3 is model 2 with further adjustment for biopsy status and biopsy status × time interaction. Model 4 is model 3 with further adjustment for age, gender, diabetes status, and rejection history. Time is measured in years.

ACR, albumin-to-creatinine ratio; eGFR, estimated glomerular filtration rate; MRE, magnetic resonance elastography.

ACR × time interaction term (to control for the prognostic effects of baseline albuminuria) and follow-up time (model 2), finding that stiffness remained significantly negatively associated with eGFR change over time ($\beta = -0.50$, $P < 0.005$). As patients undergoing a clinically indicated biopsy likely differ from nonbiopsied patients at baseline and in their future renal function trajectory, we further adjusted for baseline biopsy status and biopsy status × time interaction (model 3). Even with these adjustments, stiffness remained associated with eGFR change over time ($\beta = -0.46$, $P < 0.05$) a finding that persisted when additional variables (age, gender, diabetes status, and rejection history) were included (model 4: $\beta = -0.47$,

$P < 0.05$). As expected, in all adjusted models, baseline eGFR, follow-up time, and baseline ACR × time interaction were significantly associated with future eGFR changes.

To address whether MRE-derived stiffness provides additive prognostic value on top of standard clinical variables, we next compared a model composed of these variables (model 1) with a model that also included stiffness (model 2). As shown in Table 5, the addition of stiffness improved the ability to prognosticate future eGFR change (model 2 versus model 1, AIC difference = -6.1, $G^2 = -8.1$, $P = 0.0043$). After adding biopsy status and biopsy status × time interaction term to models 1 and 2, the model with stiffness (model 4) remained a significantly better fit compared with the model without it (Table 5; model 4 versus model 3, AIC difference = -4.0, $G^2 = -2.0$, $P = 0.0455$). Further inclusion of age, gender, diabetes status, and rejection history in models 3 and 4 revealed that the model including stiffness was significantly better compared with the model without stiffness (Table 5; model 6 versus model 5, AIC difference = -4.1, $G^2 = -2.1$, $P = 0.0421$).

DISCUSSION

Despite decades of intensive research, our ability to prognosticate renal outcomes in kidney transplant recipients remains poor. Currently, transplant physicians rely on clinical biomarkers that are either nonspecific (eg, serum creatinine), or invasive and potentially at risk for sampling bias (eg, biopsy). Here, we evaluated the use of allograft MRE as a way to noninvasively assess dysfunctional allograft injury. We found that higher renal MRE-derived stiffness scores associated with more rapid decline in allograft function over time, irrespective of baseline clinical measures and biopsy status. Our findings suggest that MRE may be a useful adjunctive imaging test, which could be performed in addition to a renal biopsy, in the workup of a patient with allograft dysfunction.

To our knowledge, our study is the largest of its kind. Importantly, we also had access to extensive follow-up renal function data, including a mean of 13 ± 9 eGFR values per

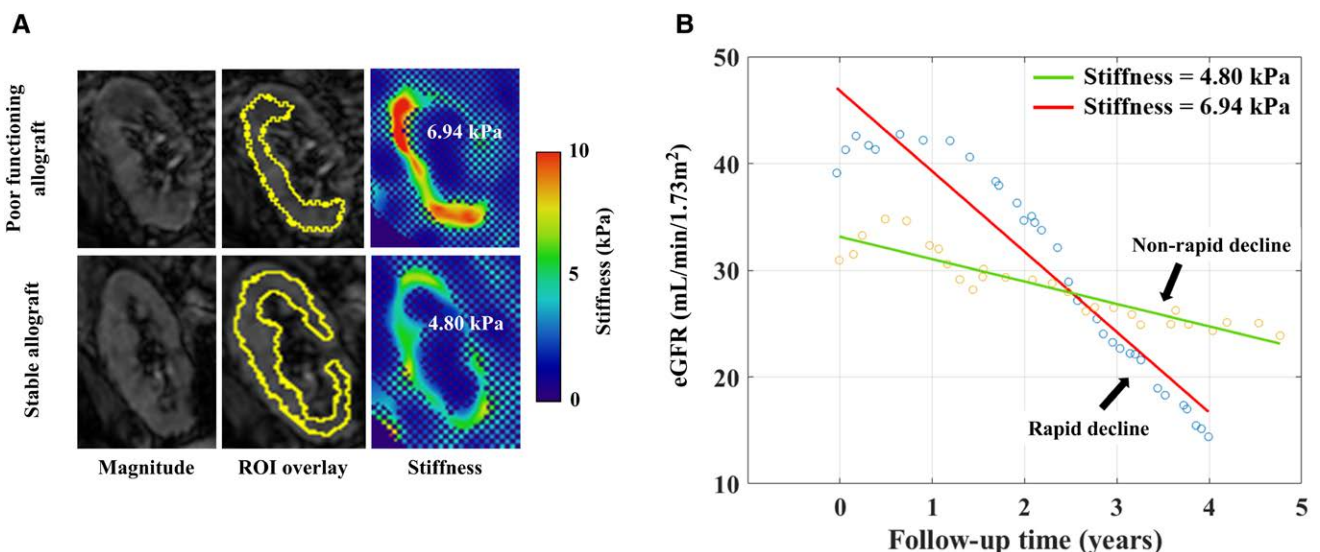


FIGURE 4. Stiffness is associated with rapid functional decline. (A) Representative MRE-derived magnitude, ROI, and stiffness maps of 2 sample kidney allografts from our cohort. Cooler and warmer colors represent softer and stiffer tissues, respectively. (B) Shown are the same 2 allografts within a baseline eGFR range of 10 mL/min/1.73m² but with different eGFR declines postscan, illustrating the relationship between stiffness and eGFR slope. eGFR, estimated glomerular filtration rate; MRE, magnetic resonance elastography; ROI, region of interest.

TABLE 5.

Stiffness provides additive information when combined with standard clinical variables as a prognostic factor for eGFR change over time using linear mixed-effects modeling

Models	Estimate of fixed effects					
	1	2	3	4	5	6
MRE-stiffness (kPa) × time		−0.495 ^a		−0.466 ^b		−0.472 ^b
Baseline eGFR (mL/min/1.73m ²)	0.864 ^c	0.862 ^c	0.870 ^c	0.869 ^c	0.877 ^c	0.875 ^c
Baseline ACR	−0.002	−0.008	−0.005	−0.007	−0.006	−0.008
Baseline ACR × time	−0.033 ^c	−0.022 ^a	−0.025 ^c	−0.021 ^a	−0.025 ^c	−0.022 ^a
Follow-up time	1.586 ^a	1.546 ^a	1.624 ^a	1.616 ^a	1.559 ^a	1.555 ^a
Biopsy status			0.666	−0.590	1.014	−0.271
Biopsy status × time			−2.166 ^b	−0.300	−2.149 ^b	−0.255
Age (y)					0.062	0.062
Gender					−0.288	−0.361
Diabetes status					1.077	1.077
Rejection history					0.144	0.124
−2log likelihood	5412.3	5404.2	5407.9	5403.9	5405.1	5401.0
AIC	5430.3	5424.2	5429.9	5427.9	5435.1	5433.0
G ²		−8.1		−4.0		−4.1
Change in AIC		−6.1		−2.0		−2.1
P value comparing the preceding model (chi-square test)		0.0043		0.0455		0.0421

^a*P* < 0.005.

^b*P* < 0.05.

^c*P* < 0.0001.

Model 1 adjusts for baseline clinical variables. Model 2 is Model 1 with further inclusion of stiffness × time interaction. Model 3 is model 1 with further inclusion of biopsy status and biopsy status × time interaction. Model 4 is model 3 with further inclusion of stiffness. Model 5 is model 3 with further inclusion of age, gender, diabetes status, and rejection history. Model 6 is model 5 with further inclusion of stiffness. Time is measured in years.

ACR, albumin-to-creatinine ratio; AIC, Akaike information criterion; eGFR, estimated glomerular filtration rate; MRE, magnetic resonance elastography.

subject over an average follow-up of over 2 y, allowing us to better assess the prognostic ability of baseline MRE scanning. Our analyses show that a single baseline contrast-free MRE scan provides information over and above what is provided by current clinical parameters, enabling more accurate prognostication of future renal function changes. Moreover, this relationship holds even when biopsy status and other clinical variables were included as covariates, suggesting that MRE may be useful in all patients with allograft dysfunction, regardless of whether a biopsy is felt to be required. Our model comparisons reveal that inclusion of stiffness in a baseline clinical model composed of baseline eGFR, ACR, and follow-up time improves the prognostication of eGFR decline, a finding that remained significant even when other relevant clinical and demographic variables were added. Thus, our findings suggest that a single MRE scan provides useful prognostic information for patients with allograft dysfunction.

MRI-based elastography has been primarily tested in, and used clinically for, imaging of liver stiffness as a surrogate measure of hepatic fibrosis and inflammation.^{28,29} We and others have recently begun exploring renal elastography as a way to image these same processes in the kidney.^{17–19,30,31} In a pilot study, we found a positive correlation between interstitial fibrosis and allograft stiffness in a small cohort of renal transplant recipients.¹⁷ These results, which are in line with those of other studies,¹⁸ suggested that, at least in some instances, kidney fibrosis contributes to stiffness. Additionally, others have suggested that perfusion is another important contributor to renal stiffness.^{19,30,31} To our knowledge, however, no MRE studies have examined inflammation as a cause of renal stiffening, despite its importance. Comparing 38 allograft scans with contemporaneously obtained biopsies, we found that MRE-derived stiffness was increased in kidneys

with microvascular inflammation (g+ptc), but not those with pure nonvascular tubular or interstitial inflammatory infiltrates (t+i). As capillaritis results in increased microvascular permeability,^{12–14} it is tempting to speculate that capillary leak-induced edema and increased renal turgor pressure may be at least partly responsible for the association between stiffness and g+ptc scores. Our results are in line with a recent study of renal transplant recipients undergoing protocol biopsies and ultrasound elastography, in which stiffness also correlated with microvascular inflammation.³²

Ultimately, multiple processes, such as microvascular inflammation, fibrosis, and perfusion, likely contribute to allograft stiffness, with the exact effects of each factor depending on the specific context. Clearly, future work will be required to tease out the settings that lead to the predominance of 1 factor over the others. In this regard, it is interesting to note that techniques that may allow separation of the individual contributions of inflammation, fibrosis, and perfusion to organ stiffness have recently been described.^{33,34} Moreover, other MRI-based techniques, such as diffusion weighted imaging, native T1 mapping and late gadolinium enhancement, have been used in the kidney or other organs to study fibrosis or inflammation.^{35–39} Finally, other nonimaging-based biomarkers may also be helpful in understanding the types of injury occurring in the kidney.^{40,41} Thus, it may be possible in the future to distinguish between the effects of each process on overall organ stiffness with a single multiparametric scanning session, with or without the use of adjunctive biomarker testing.

Importantly, our findings do not indicate that MRE scanning should replace a biopsy, as the biopsy provides critical information beyond the presence of microvascular inflammation, including the identification of tubulitis and other causes

of allograft dysfunction. Rather, our results suggest that MRE scanning may be a useful test that *supplements* the biopsy, by providing important prognostic information that is currently not generated by tissue analysis or other standard tests for allograft dysfunction.

Our study has several limitations. First, stiffness maps were reconstructed using a commercial 2D inversion algorithm. 3D reconstruction may provide more precision, by better accounting for the complex, 3D structural variations within the kidney, which collectively are termed anisotropy. Second, we used a 2D GRE-based MRE sequence, which acquires only a single slice/scan (increasing the total scan time), and is more prone to T2* decay, leading to signal loss. Despite these limitations, we were still able to achieve reproducible, high-quality images using our GRE-based technique because of the superficial location of kidney allografts, causing minimal signal attenuation.⁴² Third, we did not take post-biopsy therapies into account, which could alter an individual's renal function trajectory, particularly in individuals who are successfully treated with antirejection therapies, and thus experience improvement in allograft function. In such patients, MRE-derived stiffness measurements would potentially lose their prognostic value. Nonetheless, we included all subjects to best mimic the pretreatment scenario that clinicians face when assessing a patient with allograft dysfunction. Finally, although we observed a significantly positive correlation between stiffness and MAKE (Table S2, SDC, <http://links.lww.com/TXD/A425>; Spearman $\rho=0.30$, $P=0.01$), our sample size was modest (25 events) and thus did not have sufficient statistical power to test for the added benefit of MRE, when combined with standard clinical measures, to prognosticate MAKE (Table S2, SDC, <http://links.lww.com/TXD/A425>). Clearly, future work, involving larger cohort sizes and longer follow-up, will be required to test whether "stiffness" can be used as a prognostic factor for ESRD or death from renal causes (MAKE).

In summary, our results suggest that stiffness, as measured by MRE, a noninvasive, contrast agent-free imaging tool, may be an important factor that can prognosticate future renal function changes. Importantly, our results remained significant even when controlling for important clinical factors such as baseline eGFR and urinary albumin excretion. In patients who underwent biopsy, MRE-derived stiffness associated strongly with microvascular inflammation, suggesting that allograft stiffening may be driven at least in part by capillaritis. Future studies enrolling larger patient numbers and using augmented MRE sequences will be needed to confirm this result, and to better understand the relative contributions of different pathologic processes to allograft stiffness.

ACKNOWLEDGMENTS

We thank technologists Anthony Sheen and Cindy Hamid for performing the research MRI scans, and research staff Lindita Rapi, Weiqu Yuan, Niki Dacouris, Tiffany Thai, and Michelle Nash for assistance in protocol development, ethics board approvals, patient recruitment, data management, and study coordination. We also wish to thank Drs Ramesh Prasad and Jeffrey Zaltzman for facilitating patient recruitment from their busy transplant clinics, and Drs Andrew Common, Danny Marcuzzi, and Vikram Prabhudesai for performing all allograft biopsies. Dr Darren Yuen was supported

by a KRESCENT New Investigator and Canadian Diabetes Association Clinician Scientist salary support award and is a recipient of a CIHR New Investigator Award.

REFERENCES

1. United States Renal Data. 2018 USRDS annual report: epidemiology of kidney disease in the United States. *Am J Kidney Dis.* 2019;73:A7–A8.
2. Stegall MD, Gaston RS, Cosio FG, et al. Through a glass darkly: seeking clarity in preventing late kidney transplant failure. *J Am Soc Nephrol.* 2015;26:20–29.
3. Matas AJ, Fieberg A, Mannon RB, et al. Long-term follow-up of the DeKAF cross-sectional cohort study. *Am J Transplant.* 2019;19:1432–1443.
4. Lefaucheur C, Gosset C, Rabant M, et al. T cell-mediated rejection is a major determinant of inflammation in scarred areas in kidney allografts. *Am J Transplant.* 2018;18:377–390.
5. Nankivell BJ, Shingde M, Keung KL, et al. The causes, significance and consequences of inflammatory fibrosis in kidney transplantation: the Banff i-IFTA lesion. *Am J Transplant.* 2018;18:364–376.
6. Mengel M, Reeve J, Bunnag S, et al. Scoring total inflammation is superior to the current Banff inflammation score in predicting outcome and the degree of molecular disturbance in renal allografts. *Am J Transplant.* 2009;9:1859–1867.
7. Loupy A, Suberbielle-Boissel C, Hill GS, et al. Outcome of sub-clinical antibody-mediated rejection in kidney transplant recipients with preformed donor-specific antibodies. *Am J Transplant.* 2009;9:2561–2570.
8. Wiebe C, Gibson IW, Blydt-Hansen TD, et al. Evolution and clinical pathologic correlations of de novo donor-specific HLA antibody post kidney transplant. *Am J Transplant.* 2012;12:1157–1167.
9. Parajuli S, Redfield RR, Garg N, et al. Clinical significance of microvascular inflammation in the absence of anti-HLA DSA in kidney transplantation. *Transplantation.* 2019;103:1468–1476.
10. Gupta A, Broin PÓ, Bao Y, et al. Clinical and molecular significance of microvascular inflammation in transplant kidney biopsies. *Kidney Int.* 2016;89:217–225.
11. Sis B, Jhangri GS, Riopel J, et al. A new diagnostic algorithm for antibody-mediated microcirculation inflammation in kidney transplants. *Am J Transplant.* 2012;12:1168–1179.
12. Doreille A, Dieudé M, Cardinal H. The determinants, biomarkers, and consequences of microvascular injury in kidney transplant recipients. *Am J Physiol Renal Physiol.* 2019;316:F9–F19.
13. Bábíčková J, Klinkhammer BM, Buhl EM, et al. Regardless of etiology, progressive renal disease causes ultrastructural and functional alterations of peritubular capillaries. *Kidney Int.* 2017;91:70–85.
14. Yamamoto I, Horita S, Takahashi T, et al. Caveolin-1 expression is a distinct feature of chronic rejection-induced transplant capillaropathy. *Am J Transplant.* 2008;8:2627–2635.
15. Leung G, Kirpalani A, Szeto SG, et al. Could MRI be used to image kidney fibrosis? A review of recent advances and remaining barriers. *Clin J Am Soc Nephrol.* 2017;12:1019–1028.
16. Muthupillai R, Lomas DJ, Rossman PJ, et al. Magnetic resonance elastography by direct visualization of propagating acoustic strain waves. *Science.* 1995;269:1854–1857.
17. Kirpalani A, Hashim E, Leung G, et al. Magnetic resonance elastography to assess fibrosis in kidney allografts. *Clin J Am Soc Nephrol.* 2017;12:1671–1679.
18. Lee CU, Glockner JF, Glaser KJ, et al. MR elastography in renal transplant patients and correlation with renal allograft biopsy: a feasibility study. *Acad Radiol.* 2012;19:834–841.
19. Kennedy P, Bane O, Hectors SJ, et al. Magnetic resonance elastography vs. point shear wave ultrasound elastography for the assessment of renal allograft dysfunction. *Eur J Radiol.* 2020;126:108949.
20. Cockfield SM, Wilson S, Campbell PM, et al. Comparison of the effects of standard vs low-dose prolonged-release tacrolimus with or without ACEi/ARB on the histology and function of renal allografts. *Am J Transplant.* 2019;19:1730–1744.
21. Levey AS, Stevens LA, Schmid CH, et al; CKD-EPI (Chronic Kidney Disease Epidemiology Collaboration). A new equation to estimate glomerular filtration rate. *Ann Intern Med.* 2009;150:604–612.
22. Silva AM, Grimm RC, Glaser KJ, et al. Magnetic resonance elastography: evaluation of new inversion algorithm and quantitative analysis method. *Abdom Imaging.* 2015;40:810–817.

23. Solez K, Colvin RB, Racusen LC, et al. Banff 07 classification of renal allograft pathology: updates and future directions. *Am J Transplant.* 2008;8:753–760.
24. Kasiske BL, Vazquez MA, Harmon WE, et al. Recommendations for the outpatient surveillance of renal transplant recipients. American Society of Transplantation. *J Am Soc Nephrol.* 2000;11 (Suppl 15):S1–S86.
25. Leffondre K, Boucquemont J, Tripepi G, et al. Analysis of risk factors associated with renal function trajectory over time: a comparison of different statistical approaches. *Nephrol Dial Transplant.* 2015;30:1237–1243.
26. Hallan SI, Ritz E, Lydersen S, et al. Combining GFR and albuminuria to classify CKD improves prediction of ESRD. *J Am Soc Nephrol.* 2009;20:1069–1077.
27. Baker RJ, Mark PB, Patel RK, et al. Renal association clinical practice guideline in post-operative care in the kidney transplant recipient. *BMC Nephrol.* 2017;18:174.
28. Rouvière O, Yin M, Dresner MA, et al. MR elastography of the liver: preliminary results. *Radiology.* 2006;240:440–448.
29. Arena U, Vizzutti F, Corti G, et al. Acute viral hepatitis increases liver stiffness values measured by transient elastography. *Hepatology.* 2008;47:380–384.
30. Garcia SRM, Fischer T, Dürr M, et al. Multifrequency magnetic resonance elastography for the assessment of renal allograft function. *Invest Radiol.* 2016;51:591–595.
31. Warner L, Yin M, Glaser KJ, et al. Noninvasive In vivo assessment of renal tissue elasticity during graded renal ischemia using MR elastography. *Invest Radiol.* 2011;46:509–514.
32. Carrera LB, Alquicira JB. MO937: Association of renal elastography with Banff microvascular inflammation in protocol biopsies for subclinical renal graft rejection diagnosis. *Nephrol Dial Transplant.* 2021;36:gfab110.0016.
33. Yin M, Glaser KJ, Manduca A, et al. Distinguishing between hepatic inflammation and fibrosis with MR elastography. *Radiology.* 2017;284:694–705.
34. Brown RS, Sun MRM, Stillman IE, et al. The utility of magnetic resonance imaging for noninvasive evaluation of diabetic nephropathy. *Nephrol Dial Transplant.* 2020;35:970–978.
35. Puntmann VO, Peker E, Chandrasekhar Y, et al. T1 mapping in characterizing myocardial disease: a comprehensive review. *Circ Res.* 2016;119:277–299.
36. Togao O, Doi S, Kuro-o M, et al. Assessment of renal fibrosis with diffusion-weighted MR imaging: study with murine model of unilateral ureteral obstruction. *Radiology.* 2010;255:772–780.
37. Buchanan CE, Mahmoud H, Cox EF, et al. Quantitative assessment of renal structural and functional changes in chronic kidney disease using multi-parametric magnetic resonance imaging. *Nephrol Dial Transplant.* 2020;35:955–964.
38. Li Q, Li J, Zhang L, et al. Diffusion-weighted imaging in assessing renal pathology of chronic kidney disease: a preliminary clinical study. *Eur J Radiol.* 2014;83:756–762.
39. Zhao J, Wang ZJ, Liu M, et al. Assessment of renal fibrosis in chronic kidney disease using diffusion-weighted MRI. *Clin Radiol.* 2014;69:1117–1122.
40. Schmidt IM, Sarvode Mothi S, Wilson PC, et al. Circulating plasma biomarkers in biopsy-confirmed kidney disease. *Clin J Am Soc Nephrol.* 2022;17:27–37.
41. Srivastava A, Schmidt IM, Palsson R, et al. The associations of plasma biomarkers of inflammation with histopathologic lesions, kidney disease progression, and mortality—The Boston Kidney Biopsy Cohort Study. *Kidney Int Rep.* 2021;6:685–694.
42. Venkatesh SK, Ehman RL. Magnetic resonance elastography of abdomen. *Abdom Imaging.* 2015;40:745–759.